Available online at www.sciencedirect.com
ScienceDirect
Biomaterials 28 (2007) 1798–1805
Biomaterials
www.elsevier.com/locate/biomaterials

Analysis of ectopic and orthotopic bone formation in cell-based tissue-engineered constructs in goats

Moyo C. Kruyt[a,*], Wouter J.A. Dhert[a], F. Cumhur Oner[a], Clemens A. van Blitterswijk[b], Abraham J. Verbout[a], Joost D. de Bruijn[b,c]

[a]*Department of Orthopaedics, G05.228, University Medical Center Utrecht, P.O. Box 85500, 3508 GA Utrecht, The Netherlands*
[b]*Institute for Biomedical Technology, Twente University Enschede, The Netherlands*
[c]*Queen Mary University of London, Mile End Road, London, UK*

Received 5 October 2006; accepted 29 November 2006
Available online 19 December 2006

Abstract

Despite decades of extensive research, the application of cell-based bone tissue engineering in clinically relevant models remains challenging. To improve effectiveness, a better understanding of how the technique should work is crucial. In the current study, we investigated the onset time, rate, location and direction of bone formation in ectopically and orthotopically implanted clinically sized tissue-engineered constructs to gain insight the mechanism behind it. Bone marrow stromal cells (BMSCs) were obtained from 10 goats, culture expanded and cryopreserved. Porous biphasic calcium phosphate (BCP) disks of 17 mm × 6 mm were per-operatively seeded with BMSCs or left empty. Both conditions were implanted intramuscularly and in bilateral critical-sized iliac wing defects. Fluorochromes were administered at 3, 5 and 7 weeks and samples were retrieved after 9 weeks. Histology showed abundant and homogeneous bone formation throughout the intramuscular BMSC samples and little bone in the controls. Histomorphometry and measurements of the fluorochrome labels of the ectopical BMSC samples indicated that osteogenesis started at the periphery and subsequent osteoconduction filled the whole scaffold within 7 weeks. In the orthotopically implanted disks, there was good integration with the surrounding bone, but minimal bone in the center of the implants, in both conditions. Bone was only derived from the interface with the surrounding bone, there was no early bone at the surfaces in contact to soft tissue as was seen in the ectopical samples. Apparently cell survival was minimal and insufficient for relevant additional bone formation. However, the speed of integration with surrounding bone and subsequent bone apposition on the BMSC-seeded orthotopic scaffolds were found to be significantly enhanced, which may be relevant especially in challenging environments.

Keywords: Bone tissue engineering; Stem cells; Goats; Polychrome labeling; Cell survival

1. Introduction

For decades, bone tissue engineering (TE), by combining bone marrow stromal cells (BMSCs) with porous scaffolds, has been explored as an alternative for the autologous bone graft. Despite considerable achievements in small animal models, little progress has been made with respect to clinical application. In fact, no randomized clinical trials have been reported so far. One of the main problems is the lack of understanding of how the technique should work using clinically sized grafts. Although some authors foresee the problem of impaired cell survival for cell-derived osteogenesis, in grafts exceeding the cubic millimeter scale [1,2], most scientists ignore this dilemma and presume the mechanism to be cell-derived osteogenesis, similarly to what is shown in small implants in rodents [3,4]. Based on the scarce literature, the acceptable distance for diffusion of oxygen and nutrients ranges from 100 μm to 1 mm [1,5], which is usually exceeded by the larger size of clinically applied bone grafts. Therefore, unless other mechanisms play a role in

*Corresponding author. Tel.: +31 30 2506971; fax: +31 30 2510638.
E-mail address: mkruyt@umcutrecht.nl (M.C. Kruyt).

0142-9612/$ - see front matter © 2006 Elsevier Ltd. All rights reserved.
doi:10.1016/j.biomaterials.2006.11.038

addition to the limited cell-derived osteogenesis, cell-based bone TE may not be feasible for clinical application. Such alternative mechanisms could be either osteoinduction or osteoconduction, which are already well-established mechanisms of bone formation. Because at least some reports do indicate an effect of BMSCs in clinically sized implants both orthotopically and ectopically [6–9], these alternative mechanisms may be enhanced or stimulated by these cells. The hypothesis that BMSC-derived bone formation relies not only on localized osteogenesis, but is more complicated may also be supported by the findings with 7 mm diameter cubic constructs in our intramuscular goat model. Although these constructs required viable BMSCs at implantation in order to yield bone, at the periphery where most cell survival would be expected, actually less bone was observed than in the interior [10].

In the previous studies on ectopic bone formation, constructs that were seeded per-operatively with cryopreserved cells, scaffolds that were pre-incubated for several hours and constructs that were 1-week pre-cultured showed comparable bone yields [10,11]. Although pre-culturing seems advantageous to stimulate osteogenic differentiation, a dense cell layer forms on the outside that may negatively influence diffusion and vascularization into the construct. That could have been the reason why no relevant effect of BMSCs was found in a study where we investigated the effect of 1-week pre-cultured BMSC constructs in an iliac wing defect model [8]. In the current study, we therefore used per-operatively seeded constructs to investigate bone formation both ectopically and orthotopically.

To discriminate between the three different established mechanisms of bone formation, the onset time of bone formation in relation to the location is crucial. Osteogenesis (by surviving BMSCs) can be expected to occur early, before 3 weeks after implantation [4,12]. Material-directed osteoinduction, possibly by adhering factors, will start later, as this phenomenon has not been reported before 4-week implantation [13–15]. Finally, osteoconduction from surrounding host bone or already established BMSC-derived bone inside the construct, will show directional bone migration, i.e. spread over the scaffold surface [16,17].

A well-known method to study the dynamics of bone formation is sequential fluorochrome labeling. These labels bind to free Ca^{2+} and are incorporated in the mineralizing bone. The label is excreted rapidly and unlabeled bone formation continues until the next label is administered. By using different colors, the direction and speed can be deduced [18–20]. In this study we investigated bone formation, intramuscularly and in an iliac wing defect, in per-operatively prepared constructs of porous ceramics with or without undifferentiated BMSCs. Particular attention was given to the growth dynamics to elucidate the underlying mechanisms of (cell-based) bone formation.

2. Materials and methods

2.1. Experimental design

Institutional animal care committee approval was obtained for a study in 10 adult Dutch milk goats. Bone marrow was harvested from each goat. The BMSCs were culture expanded for two passages and then cryopreserved. During surgery, thawed, autologous BMSCs were loaded on two porous biphasic calcium phosphate (BCP) disks. Another two disks were treated similarly but without BMSC administration. Per goat one BMSC-loaded and one empty control were implanted into a bilateral critical-sized iliac wing defect. The remaining two disks were implanted in the paraspinal muscles. To monitor the bone formation in time, fluorochrome markers were administered at 3, 5 and 7 weeks and the animals were sacrificed after 9 weeks. Bone formation was investigated by histology, fluorescence microscopy and histomorphometry.

2.2. Scaffolds

BCP scaffolds (IsoTis Orthobiologics, Irvine, USA), with an 80/20 weight percent ratio of hydroxyapatite (HA) to tricalcium phosphate (TCP), sintered at 1200 °C, approximately 65% porous, and with a pore size of 200–800 μm were used. Previously, these scaffolds have been characterized by X-ray diffraction and Fourier transform infrared spectrometry and have shown to be osteoinductive without administration of inductive factors. In contrast to pure HA scaffolds, these BCP scaffolds have shown to be apt for cell-based bone TE in goats [10,21–23]. Disks of $\varnothing 17 \times 6$ mm were cut, cleaned in ultrasonic baths and steam-sterilized.

2.3. BMSCs culture and seeding conditions

After approval of the local animal care committee, 10 adult female Dutch milk goats (24–36 months) were obtained at least 4 weeks prior to surgery. Bone marrow was aspirated (15 ml per iliac wing) and analyzed for the colony-forming unit efficiency (CFUE) as previously described [24]. Simultaneously, 100 ml venous blood for the preparation of autologous serum (AS) was derived [10]. The BMSCs were culture expanded for two passages and aliquots of 10^7 BMSCs were cryopreserved in medium containing 30% fetal bovine serum (FBS, Gibco, Paisly, Scotland) and 10% dimethylsulfoxide (DMSO, Sigma, The Netherlands). At the day of surgery, two aliquots of cryopreserved cells per goat were thawed on ice, thoroughly washed with AS and resuspended in 10 ml iced AS per aliquot. Cell viability was assessed by trypan blue exclusion. During surgery, the cell suspensions were centrifuged at 300*g*, and the BMSC pellets were resuspended in 1.3 ml autologous plasma that had been derived by ultracentrifugation (1200*g*) of 10 ml peripheral blood [10]. Per goat, two disks were impregnated, each with a 1.3 ml suspension containing 10^7 autologous BMSCs ($8 \times 10^6/cm^3$) that were seeded equally on both sides of the disk. Another two disks were similarly impregnated with 1.3 ml plasma without cells (controls). After the plasma had polymerized, the samples were implanted. Additional cell seeded disks were prepared for in vitro analysis of cell distribution throughout the construct by methylene blue staining and scanning electron microscopy (SEM).

2.4. Animals and implantation

The surgical procedures were performed under standard conditions [8]. After shaving and disinfection of the dorsal thoracolumbar area, a central skin incision T10-L5 was made to expose the muscle fascia. The muscles were diathermally detached to expose the iliac wings. Under constant saline cooling, central guide holes were drilled before $\varnothing 17$ mm critical-sized trephine holes were made [25]. The implants were inserted press fit into the bilateral defects. Then the soft tissue was resutured or sutured back to the remaining fascia on the iliac crests. Bilateral intramuscular pockets were created by blunt dissection after separate fascia incisions in

the paraspinal muscles (T10–12). After insertion of the disks, the fascia was closed with a non-resorbable suture to facilitate localization at explantation. Additionally, the transverse processes L2–L4 were exposed for a bone augmentation model that will not be discussed in this paper [17]. The skin was closed in two layers. Postoperatively, pain relief was given by buprenorphine only (Shering-Plough, The Netherlands). The goats received sequential fluorochrome labels at 3 weeks (calcein green, 10 mg/kg intravenously, Sigma), 5 weeks (oxyteracycline, 32 mg/kg intramuscular, Engemycine, Mycofarm, The Netherlands) and 7 weeks (xylenol orange, 80 mg/kg intravenously, Sigma) [18]. At 9 weeks the animals were killed by an overdose of pentobarbital (Organon, The Netherlands) and the implants were retrieved.

2.5. Post-mortem sample acquisition, histology and histomorphometry

Explanted samples were fixated in 4% glutaraldehyde/5% paraformaldehyde, dehydrated by graded ethanol series and embedded in polymethylmethacrylate. The 6 mm thick disks were divided with a section 2.5 mm below and parallel to the circular surface and two semi-thin sections (10 μm) were made with a 300 μm sawing blade microtome (Leica, Nussloch, Germany) through the center. These slides demonstrated the relation with the surrounding iliac bone in the orthotopic grafts most favorably (Fig. 1). Then the remnants were joined with superglue to reconstruct the original disks (missing the central 1 mm). These were sectioned in the mid-axial plane to create two half disks and sections were made to allow additional evaluation of the peripheral disk surfaces that had been exposed to soft tissue (Fig. 2). Sections were either stained with methylene blue and basic fuchsin for routine histology and histomorphometry, or left unstained for epifluorescence microscopy with a light microscope (E600 Nikon, Japan) equipped with a quadruple filter block (XF57, dichroic mirror 400, 485, 558 and 640 nm, Omega filters, The Netherlands). For histomorphometry the central circular plane was used, high-resolution (300 dpi), low-magnification (10 ×) digital micrographs were made and blinded for further analysis. Using Adobe Photoshop 7.0, bone and scaffold were pseudocolored red and green, respectively. The area of interest was defined by adjusting the radius of a circle to exactly fit the explanted disk. Image analysis was performed using a PC-based system equipped with the KS400 version 3.0 software (Zeiss, Oberkochen, Germany). A custom-made program was used to measure the percentage of available scaffold perimeter in contact to bone (contact% = bone–scaffold contact length/scaffold perimeter length × 100%). The contact% was used because this is more sensitive for bone apposition, which has relatively little volume and always occurs on the material surface [8].

Fluorescence microscopy was used to determine, where in the scaffold, early (= 3 weeks) and late (5 and 7 weeks) mineralization occurred. These data enabled to deduce the direction and speed of bone formation (order and distance between the labels) [19]. In addition to the potential to determine the dynamics of a distinct spot of bone, also the dynamics of bone migration (osteoconduction) can be analyzed [17]. For example, the maximum speed of migration can be determined by measuring the maximum distance of the consecutive labels to the border with the surrounding host bone, representing the maximal integration depth at the

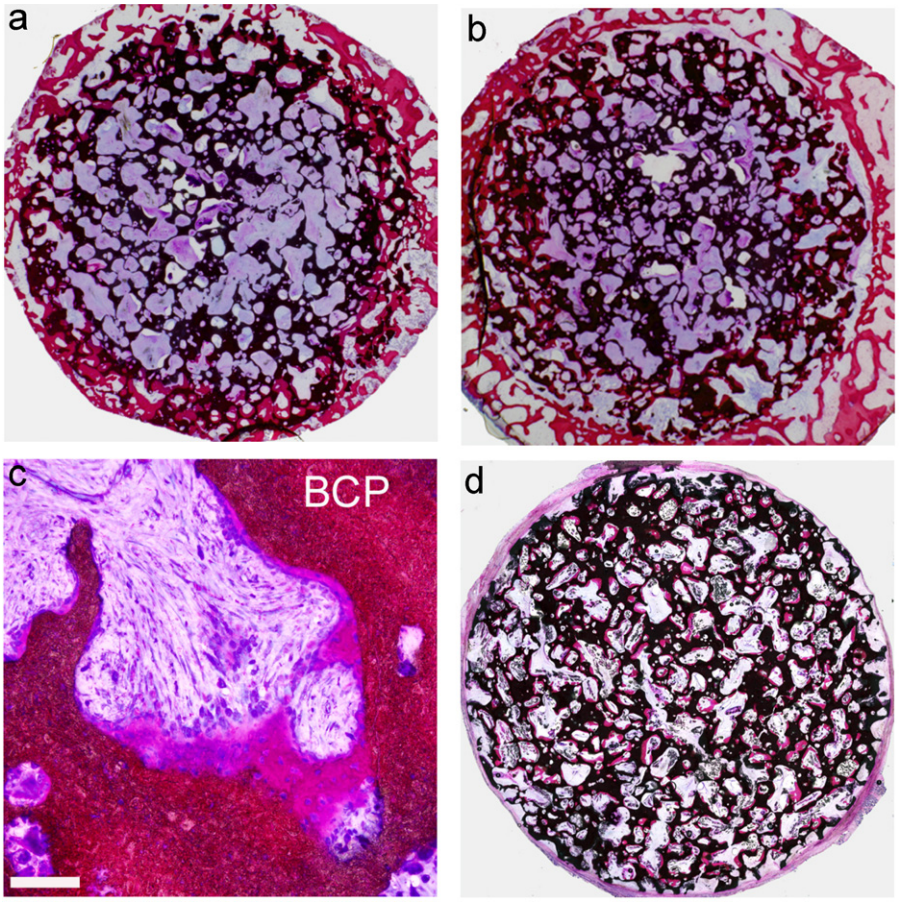

Fig. 1. Images of the circular plane of the ectopical and orthotopical implants after 9-week implantation. Bone is red, BCP scaffold is black. (a) Low magnification of the ∅17 mm orthotopical disk without BMSCs, note the well integration by the surrounding bone. (b) Low magnification of the orthotopical disk with BMSCs, note the absence of central bone formation. (c) High magnification of bone in the ectopical BCP disk without BMSCs, that is the result of the intrinsic osteoinductivity of the material (bar = 50 μm). (d) Low magnification of the ectopical disk with BMSCs, note the homogeneous distribution of bone.

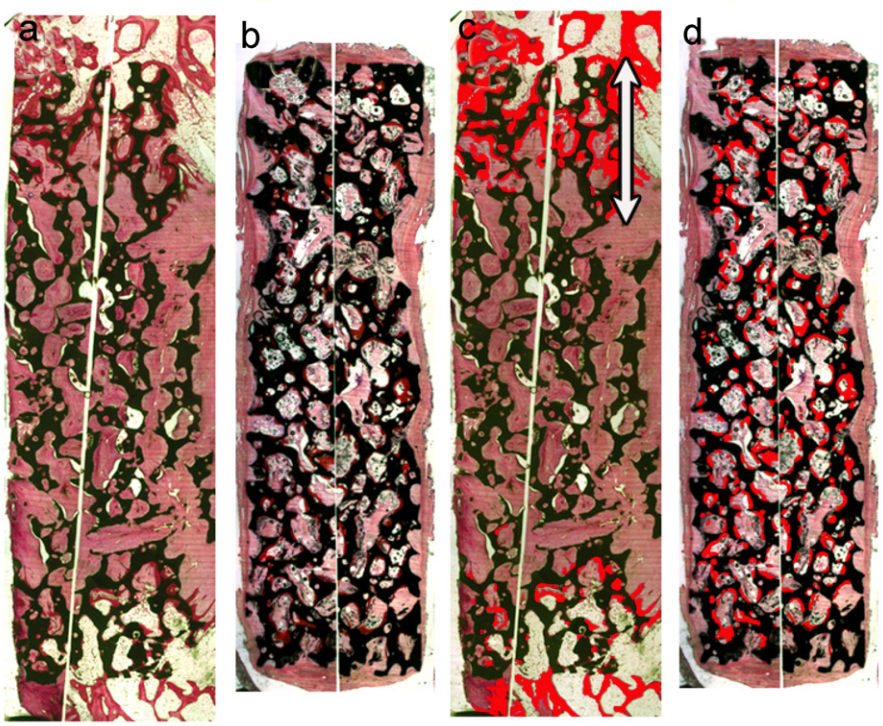

Fig. 2. Images of the mid-axial plane of the reconstructed original $\varnothing 17 \times 6$ mm disks. (a) Low magnification image of disk with BMSCs in the orthotopical condition. (b) Low magnification image of disk with BMSCs intramuscularly. (c) Pseudocolored version of (a), to highlight the bone (red). Note that there is no bone in the center of this disk. Arrow (= 4.6 mm) represents the maximum distance of bone integration after 9 weeks from one of the two outer surfaces in contact to the iliac bone. There is little bone close to the soft tissue surfaces. (d) Pseudocolored version of (b). Bone is distributed homogeneously, although not on the outside of the scaffold.

time of fluorochrome administration. Theoretically, no directional migration is expected in the case of BMSC-derived osteogenesis, because the BMSCs are distributed throughout the whole scaffold. In this study we focused on the bone migration dynamics in the mid-axial plane of the disks. The maximal bone integration depth in time was the average of the maximal distances of each label and the bone (representing the 9-week situation) to the two opposite outer surfaces (Figs. 2 and 3). Measurements were done with the microscope cross table connected to a digital micrometer (Mitutoyo, Tokyo, Japan).

2.6. Statistics

Data were analyzed for normal (parametric) distribution and are shown as mean $\pm$ standard deviation (SD). Two-sided, paired student *t*-tests were performed to analyze differences in bone apposition (contact%) between tissue-engineered and control implants. Linear mixed models were used to determine differences in the speed of bone integration. The level of significance was set at $p = 0.05$.

3. Results

3.1. In vitro

The bone marrow aspirates contained 5.6 ± 1.5E6 nucleated cells per ml. Unexpectedly the bone marrow of one goat did not show any adherent colonies with the CFU essay. Because this goat was also scheduled for another experiment without BMSCs, we could not take another

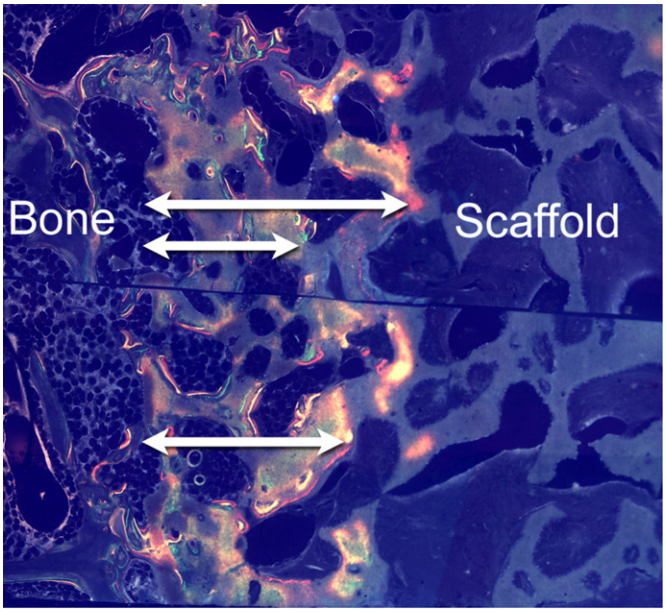

Fig. 3. Fluorescence microscopy of BMSC construct in contact to surrounding bone in the mid-axial plane. The horizontal line is the result of reconstruction of the disk of two halves (see M&M). The arrows indicate the maximal distance of the sequential labels to the scaffold bone interface: Green given at 3 weeks 1.3 mm, yellow at 5 weeks 1.8 mm and orange at 7 weeks 2.4 mm. Note the absence of bone and autofluorescence towards the center of the disk.

aspirate and excluded this goat from the study. The colony-forming efficiency of the remaining nine goats was 1.9 ± 0.6 BMSCs per 10^5 cells. Histology and SEM of the withheld constructs showed spherical cell aggregates as found in previous studies [10], throughout the entire construct, while cell densities where subjectively little higher on the periphery.

3.2. In vivo

All goats tolerated the procedures well and there were no signs of infection or other adverse reactions. The iliac wing implants were well integrated and covered with a thick, well-vascularized tissue layer. Histology of the intramuscular samples showed bone in all BMSC-seeded and control implants. This confirmed our previous findings of intrinsic osteoinductivity of the BCP material without the addition of inductive factors [8,10,26]. However, in the cell-seeded disks, much higher quantities of bone were present, always in connection to the scaffold material, homogeneously distributed, but never on the exterior of the scaffold (Figs. 1 and 2). All orthotopical samples were well integrated. Bone had grown in from the host iliac bone at various depths, reaching the center in one of nine in the control, and two of nine in the BMSC conditions. No enchondral bone formation was observed in any of the samples. Histomorphometry of the mid-circular plane showed an average macroporosity of $51 \pm 4\%$. The contact% bone showed a relatively high SD of about 30% of the mean, partially this was a result of considerable inter-goat variability that could be excluded by the paired comparisons setup. In the ectopical disks, an obvious effect of BMSCs was found. The controls showed 1.7 ± 1.2 (mean $\pm$ SD) contact% bone, compared to 19.8 ± 6.9 in the BMSC condition ($p < 0.01$) (Fig. 4). Orthotopically however, the BMSCs showed only marginally more bone (25.1 ± 10.3 vs. 32.9 ± 7.0, $p = 0.04$).

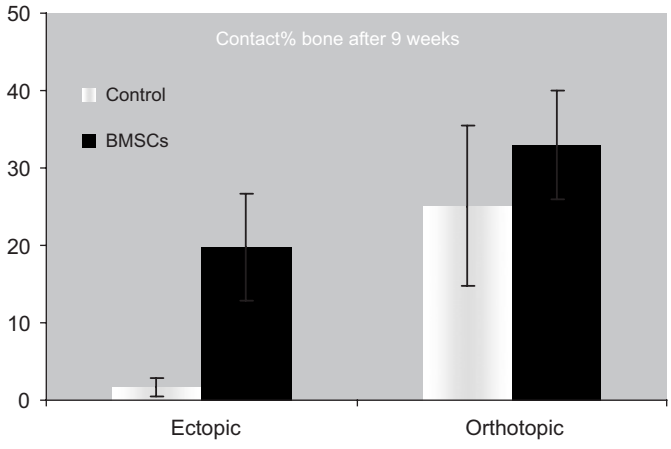

Fig. 4. Bone apposition inside the ectopical and orthotopical disks after 9 weeks (contact%). The effect of BMSCs was obvious ectopically ($p < 0.01$). Orthotopically, the effect was less pronounced, although paired measurements indicated it to be significant ($p = 0.04$). The fraction of disks that was covered with bone in the center is indicated.

Fluorescence microscopy of both the circular and axial slides of the ectopical controls occasionally showed the 7-week label, indicating mineralization of bone occurred after 5-week implantation as was expected for the osteoinductive mechanism of bone formation. Within the ectopical BMSC disks, all sequential labels were present. The early label was only seen in the periphery at a maximum depth of 1.4 ± 0.6 mm. The 5- and 7-week labels were both found throughout the samples at the maximal dept of 2.5 mm (central 1 mm was sectioned to provide the circular slides). This suggests bone mineralization initiated peripherally and covered the whole implant within 5 weeks. The orthotopical disks showed a remarkable different distribution of the labels. In both the control and BMSC conditions, the early label was only found close to the scaffold–bone interface and not near the interface with soft tissue, as was seen in the ectopical disks (Fig. 3). The sequential labels and bone (representing the 9 weeks) were found more centrally in the disks. There was an almost perfect linear relationship between label depth and time in both conditions after 3-week implantation ($R^2 = 0.98$, $p < 0.01$). The slope of this line represents the bone ingrowth speed, which appeared faster in the BMSC condition at 0.72 mm/week compared to 0.47 mm/week in the controls ($p < 0.01$, Fig. 5).

4. Discussion

In a previous study with similar constructs that had been pre-cultured for 1 week prior to implantation into the same iliac wing model, we found unsatisfactory results with respect to the effect of BMSCs [8]. Based on the promising results of others with constructs that had not been pre-cultured [6,7,27], we hypothesized that the higher cell density and dense extracellular matrix that we found on the periphery of pre-cultured constructs may have been

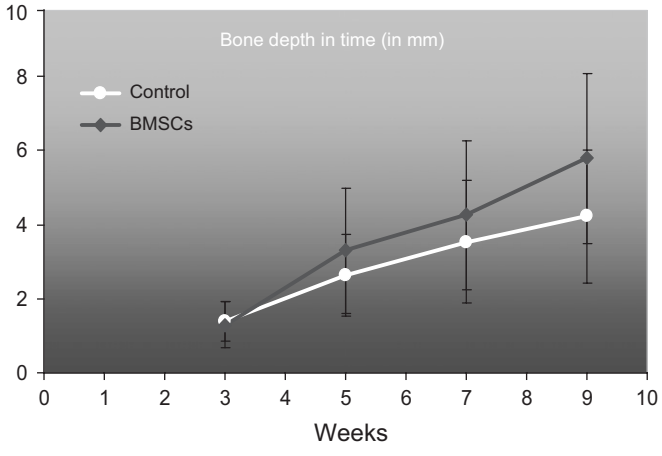

Fig. 5. Line graph indicating the maximum depth of mineralizing bone at 3, 5, 7 and 9 weeks inside the orthotopical disks. The 3-week label was at comparable depth in both the BMSC and control condition. After 3 weeks there was a strong linear relationship ($R^2 = 0.98$). In the BMSC condition, bone conduction speed was at 0.72 mm/week compared to 0.47 mm/week in the control ($p < 0.01$).

disadvantageous. Therefore, we conducted the current study with constructs that were per-operatively prepared with BMSCs in autologous blood plasma that polymerized after impregnation of the scaffold. This method has previously shown to be at least as good as seeding BMSCs that had not been cryopreserved or pre-culturing of the constructs [10,11] and was expected to minimize the immediate influx of host blood cells and therefore diminished the number of cells in competition for survival [1]. However, the results in the current study were almost similar to those in the previous study, with respect to the marginal effect of the BMSCs in the orthotopic location. The functionality of the BMSC constructs, however, was clearly shown by the 100% success rate and high bone yields in the ectopically implanted identical constructs. The homogeneous distribution of bone in these disks in contrast to the orthotopical counterparts was most remarkable, together with the finding that the onset of osteogenesis was always confined to the peripheral 2 mm. Apparently, in the ectopical samples bone started at the periphery and progressed to fill the entire disk within 5 weeks (Fig. 6). After 5 weeks, bone apposition continued on the remaining scaffold surface and on itself, which could be determined by the presence of the 7-week label and final 9-week histology. These observations may be explained by cell survival and early osteogenesis restricted to the peripheral zones, followed by osteoconduction towards the center. However, it cannot be excluded that cells survived throughout the entire scaffold. In that case, delayed central bone formation could be the consequence of delayed central vascularization. Although little is known about vascularization of porous ceramics, some reports indicate several weeks are indeed needed to vascularize distances beyond 2 mm [28–30]. In contrast to the ectopic disks, however, none of the orthotopic implants showed the 3- or 5-week label at the interface with soft tissue from where blood vessels had obviously grown into disks that were well vascularized after 9 weeks. If delayed vascularization would be the only explanation for delayed bone formation, at least the 5-week label should have been present here, inside bone generated by surviving BMSCs. Apparently, in the orthotopical condition not enough BMSCs survived for cell-based osteogenesis. This can possibly be a result of hematoma formation between the disk and overlying muscles, which increased the diffusion distance and resulted in a potassium-rich environment detrimental to cell survival [31]. However, it cannot be excluded that in addition to a less favorable wound bed, the fracture healing response itself is a negative factor as compared to the ectopical wound healing response.

Despite the apparent lack of cell survival at the soft tissue interface, there are strong indications for enhanced osteoconduction in the BMSC condition from the interface with bone. Starting after 3 weeks, the consecutive labels indicated a higher velocity of bone ingrowth (Fig. 5). Also the contact% bone after 9 weeks appeared higher. Possibly, BMSCs near the surrounding bone did survive and resulted in more early bone in the peripheral 2 mm, which finally resulted in more bone apposition after 9 weeks. However, it is difficult to conclude this because in the controls the distance of the 3-week label from the surrounding bone was similar. Alternatively the initial presence of the BMSCs stimulated bone formation later on by either stimulating vascularization [28,32,33], that is required for osteoconduction [34], or as a consequence of the release of factors [34], stimulating migration and induction of cells in the surrounding bone [35,36]. Both these mechanisms are different from the osteogenic mechanism of cell-based tissue-engineered bone formation that is generally expected, it would therefore be very valuable if the exact mechanism is investigated more routinely.

5. Conclusion

In the current study, we investigated the three main mechanisms of bone formation (i.e., osteoconduction, osteoinduction and osteogenesis), based on their onset time and growth dynamics, in BMSC-seeded and control

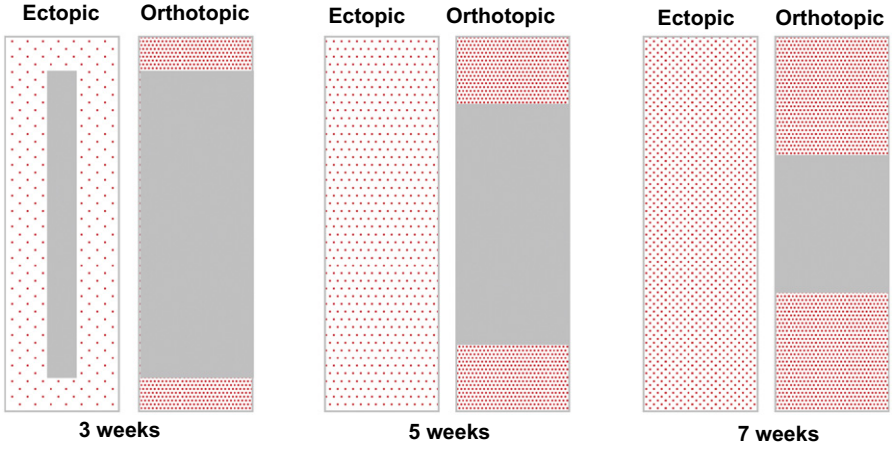

Fig. 6. Schematic cartoon of the distribution of bone in time, in the ectopical and orthotopical BMSC conditions. Slides as shown in Fig. 3. Dotted area represents the area and density of bone. Note in the ectopical samples bone is coming from the periphery and increases in time.

scaffolds in the ectopic and orthotopic environment. Ectopically, osteoinduction was observed in the control scaffolds around 5-week implantation. In the BMSC constructs, there were strong indications for earlier cell-based osteogenesis on the implant periphery and subsequent osteoconduction towards the center. In the orthotopic constructs, cell-based osteogenesis appeared to be nearly absent. Although BMSCs appeared to be favorable in stimulating osteoconduction, the likelihood that insufficient cells survive for relevant osteogenesis in clinical applications of the technique, should be recognized. Therefore, the mechanism of cell-based tissue-engineered bone formation should be elucidated in successful clinically relevant models, where it may be less dependent on cell-based osteogenesis than expected.

Acknowledgments

The authors acknowledge The Netherlands Technology Foundation (STW; Grant UGN.4966) for financial support. We also thank H. Yuan (IsoTis SA, The Netherlands) for kindly providing the BCP scaffold materials.

References

[1] Muschler GF, Nakamoto C, Griffith LG. Engineering principles of clinical cell-based tissue engineering. J Bone Joint Surg Am 2004;86-A(7):1541–58.
[2] Rose FR, Oreffo RO. Bone tissue engineering: hope vs hype. Biochem Biophys Res Commun 2002;292(1):1–7.
[3] Bruder SP, Kurth AA, Shea M, Hayes WC, Jaiswal N, Kadiyala S. Bone regeneration by implantation of purified, culture-expanded human mesenchymal stem cells. J Orthop Res 1998;16(2):155–62.
[4] Kruyt MC, Stijns MM, Fedorovich NE, De Bruijn JD, Van Blitterswijk CA, Verbout AJ, et al. Genetic marking with the DeltaLNGFR-gene for tracing goat cells in bone tissue engineering. J Orthop Res 2004;22(4):697–702.
[5] Ishaug-Riley SL, Crane GM, Gurlek A, Miller MJ, Yasko AW, Yaszemski MJ, et al. Ectopic bone formation by marrow stromal osteoblast transplantation using poly(DL-lactic-*co*-glycolic acid) foams implanted into the rat mesentery. J Biomed Mater Res 1997;36(1):1–8.
[6] Petite H, Viateau V, Bensaid W, Meunier A, de Pollak C, Bourguignon M, et al. Tissue-engineered bone regeneration. Nat Biotechnol 2000;18(9):959–63.
[7] Arinzeh TL, Peter SJ, Archambault MP, van den Bos C, Gordon S, Kraus K, et al. Allogeneic mesenchymal stem cells regenerate bone in a critical-sized canine segmental defect. J Bone Joint Surg Am 2003;85-A(10):1927–35.
[8] Kruyt MC, Dhert WJ, Yuan H, Wilson CE, van Blitterswijk CA, Verbout AJ, et al. Bone tissue engineering in a critical size defect compared to ectopic implantations in the goat. J Orthop Res 2004;22(3):544–51.
[9] Bensaid W, Oudina K, Viateau V, Potier E, Bousson V, Blanchat C, et al. De novo reconstruction of functional bone by tissue engineering in the metatarsal sheep model. Tissue Eng 2005;11(5–6):814–24.
[10] Kruyt MC, De Bruijn JD, Yuan H, Van Blitterswijk CA, Verbout AJ, Oner FC, et al. Optimization of bone tissue engineering in goats: a peroperative seeding method using cryopreserved cells and localized bone formation in calcium phosphate scaffolds. Transplantation 2004;77(3):359–65.
[11] Kruyt MC, Dhert WJ, Oner C, van Blitterswijk CA, Verbout AJ, de Bruijn JD. Optimization of bone-tissue engineering in goats. J Biomed Mater Res 2004;69B(2):113–20.
[12] Burwell RG. The function of bone marrow in the incorporation of a bone graft. Clin Orthop 1985;200(200):125–41.
[13] Yuan H, Yang Z, De Bruijn JD, De Groot K, Zhang X. Material-dependent bone induction by calcium phosphate ceramics: a 2.5-year study in dog. Biomaterials 2001;22(19):2617–23.
[14] Habibovic P, Sees TM, van den Doel MA, van Blitterswijk CA, de Groot K. Osteoinduction by biomaterials—physicochemical and structural influences. J Biomed Mater Res A 2006;77(4):747–62.
[15] Habibovic P, Yuan H, van den Doel M, Sees TM, van Blitterswijk CA, de Groot K. Relevance of osteoinductive biomaterials in critical-sized orthotopic defect. J Orthop Res 2006;24(5):867–76.
[16] Davies JE. Mechanisms of endosseous integration. Int J Prosthodont 1998;11(5):391–401.
[17] Wilson CE, Kruyt MC, de Bruijn JD, van Blitterswijk CA, Oner FC, Verbout AJ, et al. A new in vivo screening model for posterior spinal bone formation: comparison of ten calcium phosphate ceramic material treatments. Biomaterials 2006;27(3):302–14.
[18] Rahn BA, Bacellar FC, Trapp L, Perren SM. Methode zur Fluoreszenz Morphometrie des Knochenanbaus. Aktual Traumatol 1980;10:109–15.
[19] Pautke C, Vogt S, Tischer T, Wexel G, Deppe H, Milz S, et al. Polychrome labeling of bone with seven different fluorochromes: enhancing fluorochrome discrimination by spectral image analysis. Bone 2005;37(4):441–5.
[20] Roldan JC, Jepsen S, Miller J, Freitag S, Rueger DC, Acil Y, et al. Bone formation in the presence of platelet-rich plasma vs. bone morphogenetic protein-7. Bone 2004;34(1):80–90.
[21] Yuan H, Van Den Doel M, Li SH, van Blitterswijk C, De Groot K, De Bruijn JD. A comparison of the osteoinduction potential of two calcium phosphate ceramics intramuscularly in goats. J Mater Sci Mat Med 2002;13:1271–5.
[22] Kruyt MC, de Bruijn JD, Wilson CE, Oner FC, van Blitterswijk CA, Verbout AJ, et al. Viable osteogenic cells are obligatory for tissue-engineered ectopic bone formation in goats. Tissue Eng 2003;9(2):327–36.
[23] Kruyt MC, Wilson CE, de Bruijn JD, van Blitterswijk CA, Oner CF, Verbout AJ, et al. The effect of cell-based bone tissue engineering in a goat transverse process model. Biomaterials 2006;27(29):5099–106.
[24] Kruyt MC, Wilson CE, de Bruijn JD, van Blitterswijk CA, Oner CF, Verbout AJ, et al. The effect of cell-based bone tissue engineering in a goat transverse process model. Biomaterials 2006.
[25] Anderson ML, Dhert WJ, de Bruijn JD, Dalmeijer RA, Leenders H, van Blitterswijk CA, et al. Critical size defect in the goat's os ilium. A model to evaluate bone grafts and substitutes. Clin Orthop 1999;364(364):231–9.
[26] Yuan H, van Blitterswijk CA, de Groot K, de Bruijn JD. Cross-species comparison of ectopic bone formation in biphasic calcium phosphate (BCP) and hydroxyapatite (HA) scaffolds. Tissue Eng 2006;12(6):1607–15.
[27] Muschler GF, Nitto H, Matsukura Y, Boehm C, Valdevit A, Kambic H, et al. Spine fusion using cell matrix composites enriched in bone marrow-derived cells. Clin Orthop 2003;407:102–18.
[28] Pelissier P, Villars F, Mathoulin-Pelissier S, Bareille R, Lafage-Proust MH, Vilamitjana-Amedee J. Influences of vascularization and osteogenic cells on heterotopic bone formation within a madreporic ceramic in rats. Plast Reconstr Surg 2003;111(6):1932–41.
[29] Pacheco EM, Civelek AC, Natarajan TK, D'Anna SA, Iliff NT, Green WR. Clinicopathological correlation of technetium bone scan in vascularization of hydroxyapatite implants. A primate model. Arch Ophthalmol 1997;115(9):1173–7.
[30] Grenga TE, Zins JE, Bauer TW. The rate of vascularization of coralline hydroxyapatite. Plast Reconstr Surg 1989;84(2):245–9.

[31] Street J, Winter D, Wang JH, Wakai A, McGuinness A, Redmond HP. Is human fracture hematoma inherently angiogenic? Clin Orthop 2000;378(378):224–37.
[32] Al-Khaldi A, Eliopoulos N, Martineau D, Lejeune L, Lachapelle K, Galipeau J. Postnatal bone marrow stromal cells elicit a potent VEGF-dependent neoangiogenic response in vivo. Gene Ther 2003;10(8):621–9.
[33] Kaigler D, Krebsbach PH, Polverini PJ, Mooney DJ. Role of vascular endothelial growth factor in bone marrow stromal cell modulation of endothelial cells. Tissue Eng 2003;9(1):95–103.
[34] Street J, Bao M, deGuzman L, Bunting S, Peale Jr FV, Ferrara N, et al. Vascular endothelial growth factor stimulates bone repair by promoting angiogenesis and bone turnover. Proc Natl Acad Sci USA 2002;99(15):9656–61 Epub 2002 Jul 9612.
[35] Hirano H, Urist MR. Induced bone development in transplants of fresh human pseudomalignant heterotopic ossification tissue in athymic nude mice. Clin Orthop 1991;263(263):113–20.
[36] de Bruyn PH, Kabisch WT. Bone formation by fresh and frozen autogenous and homogenous transplants of bone, bone marrow and periosteum. Am J Anat 1955;96:375–417.